Inorg. Chem. **1995,** *34,* 5632−5640

Solution Chemistry and Crystal Structure of Nickel Tetrakis(2,3,5,6-tetrafluoro-*N,N,N*-trimethyl-4-aniliniumyl)porphyrin Trifluoromethanesulfonate (NiTF$_4$TMAP(CF$_3$SO$_3$)$_4$)

Timothy La, Rosalie A. Richards, Roy S. Lu, Robert Bau, and Gordon M. Miskelly*[1]

Department of Chemistry, University of Southern California, Los Angeles, California 90089-0744

Received January 27, 1995⊗

The solution chemistry and crystal structure of nickel tetrakis(2,3,5,6-tetrafluoro-*N,N,N*-trimethyl-4-aniliniumyl)porphyrin (NiTF$_4$TMAP^{4+}) are reported and compared with analogous chemistry for nickel tetrakis(N-methyl-4-pyridiniumyl)porphyrin (NiT4-N-MePyP^{4+}). NiTF$_4$TMAP^{4+} binds axial ligands more strongly than most other reported porphyrins. For stronger-field ligands such as 1-methylimidazole and tris(*n*-butyl)phosphine two sequential binding equilibria are observed, whereas with weaker ligands binding of two axial ligands appears to occur simultaneously. The four coordinate NiTF$_4$TMAP^{4+} is in equilibrium with the six coordinate Ni(H$_2$O)$_2$TF$_4$TMAP^{4+} in aqueous solution ([6 coordinate]/[4 coordinate] = 1.6), but the axial waters are readily lost in the presence of organic substrates such as aromatics (anionic and neutral) and aliphatic ligands (anionic and neutral). The interactions are best explained as being predominantly due to the hydrophobic effect. While this effect is exacerbated in this fluorinated porphyrin, these results indicate that hydrophobic effects should be considered in any study of porphyrin interactions in aqueous solution. The buffers HEPES and MES cause the porphyrin to be 4-coordinate in their basic form, but the zwitterionic forms do not interact with the porphyrin. In contrast, hydrogen phthalate displaces the coordinated water more strongly than the dibasic phthalate. These observations are probably due to increased hydration of the substrate. The crystal structure of Ni(TF$_4$TMAP)(CF$_3$SO$_3$)$_4$·2CH$_3$CN·2(CH$_3$)$_2$CO ($R = 7.59\%$, $R_w = 7.91\%$, $P\bar{1}$, $Z = 2$, $a = 14.090(3)$ Å, $b = 15.725(3)$ Å, $c = 19.554(4)$ Å, $\alpha = 78.43(3)°$, $\beta = 77.26(3)°$, $\gamma = 83.14(3)°$) showed that the nickel(II) was four coordinate, with no interactions with the anions or lattice solvent.

Introduction

The development of new water-soluble porphyrins enables researchers to probe the interactions between the porphyrin core and water in more detail than was previously possible. There are now many studies reporting the interactions of water-soluble porphyrins with DNA[2−22] and other biological substrates.[4,23−29] The characterization of the behavior of porphyrins in water is a necessary precursor to a complete understanding of the interaction of these molecules with biological substrates since most biological systems involve a predominantly aqueous medium. Previously, the interaction of porphyrins with biological molecules such as DNA and RNA has been discussed in terms of ionic bridges[30] and $\pi-\pi$ interactions.[31] We now show that a more general hydrophobic effect[32,33] can govern the behavior of porphyrins in aqueous solution. The realization that hydrophobic effects are important has been stated previously

---

⊗ Abstract published in *Advance ACS Abstracts,* September 15, 1995.

(1) Present address: Department of Chemistry, University of Auckland, Private Bag 92019, Auckland, New Zealand.

(2) Fiel, R. J.; Howard, J. C.; Mark, E. H.; Datta Gupta, N. *Nucleic Acids Res.* **1979**, *6*, 3093.

(3) Fiel, R. J.; Munson, B. R. *Nucleic Acids Res.* **1980**, *8*, 2835.

(4) Carvlin, M. J.; Mark, E.; Fiel, R.; Howard, J. C. *Nucleic Acids Res.* **1983**, *11*, 6141.

(5) Pasternack, R. F.; Gibbs, E. J.; Villafranca, J. J. *Biochemistry* **1983**, *22*, 5409.

(6) Pasternack, R. F.; Gibbs, E. J.; Villafranca, J. J. *Biochemistry* **1983**, *22*, 2406.

(7) Banville, D. L.; Marzilli, L. G.; Strickland, J. A.; Wilson, W. D. *Biopolymers* **1986**, *25*, 1837.

(8) Blom, N.; Odo, J.; Nakamoto, K.; Strommen, D. P. *J. Phys. Chem.* **1986**, *90*, 2847.

(9) Geacintov, N. E.; Ibanez, V.; Rougee, M.; Bensasson, R. V. *Biochemistry* **1987**, *26*, 3087.

(10) Strickland, J. A.; Banville, D. L.; Wilson, W., D.; Marzilli, L. G. *Inorg. Chem.* **1987**, *26*, 3398.

(11) Fiel, R. J. *J. Biomol. Struct. Dynam.* **1989**, *6*, 1259.

(12) Groves, J. T.; Farrell, T. P. *J. Am. Chem. Soc.* **1989**, *111*, 4998.

(13) Marzilli, L. G. *New J. Chem.* **1990**, *14*, 409.

(14) Sari, M. A.; Battioni, J. P.; Dupre, D.; Mansuy, D.; Le Pecq, J. B. *Biochemistry* **1990**, *29*, 4205.

(15) Yixian, L.; Koningstein, J. A.; Yevdokimov, Y. *Can. J. Chem.* **1992**, *70*, 2413.

(16) Pasternack, R. F.; Bustamante, C.; Collings, P. J.; Giannetto, A.; Gibbs, E. J. *J. Am. Chem. Soc.* **1993**, *115*, 5393.

(17) Lin, M.; Lee, M.; Yue, K. T.; Marzilli, L. G. *Inorg. Chem.* **1993**, *32*, 3217.

(18) Liu, Y.; Koningstein, J. A. *J. Phys. Chem.* **1993**, *97*, 6155.

(19) McMillin, D. R.; Liu, F.; Meadows, K. A.; Aldridge, T. K.; Hudson, B. P. *Coord. Chem. Rev.* **1994**, *132*, 105.

(20) Mukundan, N. E.; Petho, G.; Dixon, D. W.; Kim, M. S.; Marzilli, L. G. *Inorg. Chem.* **1994**, *33*, 4676.

(21) Kuroda, R.; Tanaka, H. *J. Chem. Soc., Chem. Commun.* **1994**, 1575.

(22) Sehlstedt, U.; Kim, S. K.; Carter, P.; Goodisman, J.; Vollano, J. F.; Norden, B.; Dabrowiak, J. C. *Biochemistry* **1994**, *33*, 417.

(23) Ding, L.; Casas, C.; Etemad-Moghadam, G.; Meunier, B. *New J. Chem.* **1990**, *14*, 421.

(24) Yue, K. T.; Lin, M.; Gray, T. A.; Marzilli, L. G. *Inorg. Chem.* **1991**, *30*, 3214.

(25) Pasternack, R. F.; Gibbs, E. J.; Gaudemer, A.; Antebi, A.; Bassner, S.; De Poy, L.; Turner, D. H.; Williams, A.; Laplace, F.; Lansard, M. H.; Merienne, C.; Perree-Fauvet, M. *J. Am. Chem. Soc.* **1985**, *107*, 8179.

(26) Butje, K.; Schneider, J. H.; Kim, J.-J. P.; Wang, Y.; Ikuta, S.; Nakamoto, K. *J. Inorg. Biochem.* **1989**, *37*, 119.

(27) Slama-Schwok, A.; Lehn, J.-M. *Biochemistry* **1990**, *29*, 7895.

(28) Bremard, C.; Girerd, J. J.; Merlin, J. C.; Moreau, S. *J. Mol. Struct.* **1992**, *267*, 117.

(29) Bustamente, C.; Gurrieri, S.; Pasternack, R. F.; Purrello, R.; Rizzarelli, E. *Biopolymers* **1994**, *34*, 1099.

(30) Schneider, H.-J.; Wang, M. *J. Chem. Soc., Chem. Commun.* **1994**, 413.

(31) Hunter, C. A.; Sanders, J. K. M. *J. Am. Chem. Soc.* **1990**, *112*, 5525.

(32) *The Hydrophobic Interaction Faraday Symposium*; University of Reading; The Royal Society of Chemistry: London, 1982.

(33) Ben-Naim, A. *Hydrophobic Interactions*; Plenum Press: New York, 1980.

0020-1669/95/1334-5632$09.00/0 © 1995 American Chemical Society

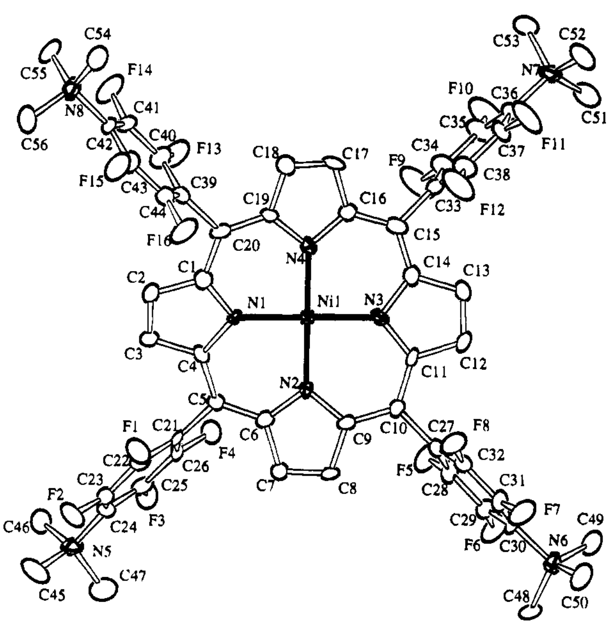

Figure 1. Diagram of the cationic porphyrin in $NiTF_4TMAP(CF_3SO_3)_4 \cdot 2CH_3CN \cdot 2(CH_3)_2CO$ showing positions of the aromatic substituents and numbering of the atoms.

for other types of DNA probes[19] and is also implicit in the observation that porphyrins with fewer than four positive charges interact more strongly with DNA than the tetracationic porphyrins.[16,34-36]

The recently reported perfluorinated porphyrin tetrakis-(2,3,5,6-tetrafluoro-*N*,*N*,*N*-trimethyl-4-aniliniumyl)porphyrin (H_2-$TF_4TMAP)^{4+}$ (Figure 1) is highly water soluble, particularly as the chloride salt, and has little propensity to dimerize, as shown by the low formation constant for formation of a (μ-oxo)iron(III) dimer ($K_D < 300\ M^{-1}$).[37] However, this porphyrin has an environment about the metal center which is best described as hydrophobic. The character of this pocket has been probed by investigating the binding of substrates to the nickel derivative. The behavior which is observed differs from that for the common synthetic water-soluble tetraarylmetalloporphyrins, in which the approach to the porphyrin face is lined with aryl hydrogens. The methyl- and chloro-substituted porphyrins developed by Bruice[38-41] and Ito[42] are expected to have similar interactions to those reported here, but equivalent chemistry for these porphyrins has not been published.

We have approached the question of ligand binding to this nickel(II) porphyrin in a systematic fashion with the intention of obtaining detailed information about both the electrophilic nature and its behavior in aqueous solutions. Thus this paper first presents results obtained with donor ligands in non-coordinating solvents for comparison with previous studies,[43-45] then examines the porphyrin behavior in donor solvents, and finally studies behavior of the nickel porphyrin in aqueous solution. The binding is described by eqs 1 and 2, although

$$MP^{n+} + L = MPL^{n+} \qquad K_1 \qquad (1)$$

$$MPL^{n+} + L = MPL_2^{\ n+} \qquad K_2 \qquad (2)$$

for weak donor molecules the two ligand additions appear simultaneous and binding is described using eq 3. This is in accord with previous studies which have reported stepwise or concerted binding of ligands to nickel porphyrins.[43-46]

$$MP^{n+} + 2L = MPL_2^{\ n+} \qquad K_1K_2 \qquad (3)$$

Experimental Section

Materials. Tri-*n*-butylphosphine, *n*-butylamine, dimethyl sulfoxide, 1-methylimidazole, and pyridine were of analytical or pure grade and were distilled immediately before use. Other solvents were analytical grade and were used as supplied except that acetonitrile for spectrophotometric studies was purified by distilling from CaH_2 under nitrogen. Water was purified using a Barnstead Nanopure system (18 MΩ cm).

Physical Measurements. Spectrophotometric measurements were performed on a Milton Roy Spectronic 3000 diode array spectrophotometer. ^1H and ^{19}F NMR were obtained on Bruker 250 and 360 MHz spectrometers. ^1H NMR data are quoted as δ(ppm) vs TMS, and ^{19}F NMR data are quoted as δ (ppm) vs $CFCl_3$. Fluorescence measurements were made using a Perkin-Elmer LS5 fluorescence spectrophotometer.

Synthesis. Tetrakis(H_2T4-N-MePyP)(4-toluenesulfonate)$_4$ (Hach) was converted to the PF_6^- salt by addition of NH_4PF_6 to an aqueous solution of the porphyrin followed by filtration. The chloride salt was then prepared by dissolution of the PF_6^- salt in acetone and addition of tetrabutylammonium chloride. The resulting chloride salt was recrystallized from acetone–water.

Ni(TF_4DMAF) and Ni(TF_4TMAP)$(CF_3SO_3)_4$ were prepared as reported previously.[37] Ni(TF_4TMAP)Cl_4 was prepared by metathesis of Ni(TF_4TMAP)$(CF_3SO_3)_4$ and tetrabutylammonium chloride in acetone at room temperature. A bright brick-red solid was obtained upon filtration. The solid was washed with acetone then diethyl ether and was air-dried. UV–vis (H_2O) 400, 420, 527, and 554 nm. ^1H NMR (D_2O) 31.8 (br, 8H, β-pyrrole), 4.16 (s, 36H, $N^+(CH_3)_3$). ^{19}F NMR (D_2O) −134.1 (s, 8F, F′), −138.1 (s, 8F, F″). No ^{19}F NMR signal from residual $CF_3SO_3^-$ was observed. Prolonged drying of the chloride salt under vacuum leads to demethylation, giving the precursor complex, Ni(TF_4DMAP).

X-ray Crystallography. Single crystals of $Ni(TF_4TMAP)(CF_3SO_3)_4 \cdot 2CH_3CN \cdot 2(CH_3)_2CO$ were grown by vapor diffusion of diethylether into a saturated solution of the nickel porphyrin (1:1 CH_3CN/acetone) in a 5 mm tube. The X-ray study was performed at the University of Southern California X-ray crystallographic center. The purple crystal of $Ni(TF_4TMAP)(CF_3SO_3)_4 \cdot 2CH_3CN \cdot 2(CH_3)_2CO$ was sealed in grease, mounted on a Siemens P4/RA automatic diffractometer, and analyzed using Cu Kα radiation monochromatized by a highly oriented graphite crystal. Data were collected at low temperature (−120 °C) to avoid solvent loss.

Three standard reflections, measured after every 100 data points, did not show any variation during data collection. Final cell constants as well as other information related to data collection and refinement are listed in Table 1. All calculations were made by using the SHELX system of crystallographic programs.[47] The structure of Ni(TF_4TMAP)-

---

(34) Butje, K.; Nakamoto, K. *Inorg. Chim. Acta* **1990**, *167*, 97.

(35) Pasternack, R. F.; Brigandi, R. A.; Abrams, M. J.; Williams, A. P.; Gibbs, E. J. *Inorg. Chem.* **1990**, *29*, 4483.

(36) Pasternack, R. F.; Giannetto, A.; Pagano, P.; Gibbs, E. J. *J. Am. Chem. Soc.* **1991**, *113*, 7799.

(37) La, T.; Richards, R.; Miskelly, G. M. *Inorg. Chem.* **1994**, *33*, 3159.

(38) Murata, K.; Panicucci, R.; Gopinath, E.; Bruice, T. C. *J. Am. Chem. Soc.* **1990**, *112*, 6072.

(39) Zipplies, M. F.; Lee, W. A.; Bruice, T. C. *J. Am. Chem. Soc.* **1986**, *108*, 4433.

(40) Panicucci, R.; Bruice, T. C. *J. Am. Chem. Soc.* **1990**, *112*, 6063.

(41) Bruice, T. C.; Zipplies, M. F.; Lee, W. A. *Proc. Natl. Acad. Sci. U.S.A.* **1986**, *83*, 4646.

(42) Ito, Y.; Kunimoto, K.; Miyachi, S.; Kako, T. *Tetrahedron Lett.* **1991**, *32*, 4007.

(43) Caughey, W. S.; Deal, R. M.; McLees, B. D.; Alben, J. O. *J. Am. Chem. Soc.* **1962**, *84*, 1735.

(44) Cole, S. J.; Curthoys, G. C.; Magnusson, E. A.; Phillips, J. N. *Inorg. Chem.* **1972**, *11*, 1024.

(45) Walker, F. A.; Hui, E.; Walker, J. M. *J. Am. Chem. Soc.* **1975**, *97*, 2390.

(46) Pasternack, R. F.; Spiro, E. G.; Teach, M. *J. Inorg. Nucl. Chem.* **1974**, *36*, 599.

(47) Sheldrick, G. M. SHELX-76, University of Cambridge. Cambridge, U. K., 1976.

(48) Sheldrick, G. M. SHELX-86, University of Gottingen. Gottingen, Germany, 1986.

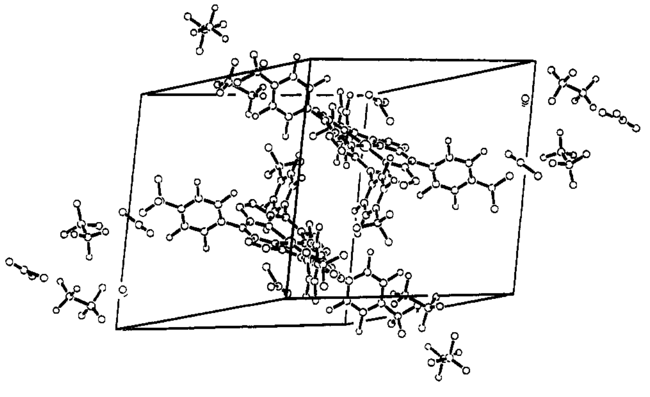

Figure 2. Diagram of the unit cell for $NiTF_4TMAP(CF_3SO_3)_4{\cdot}2CH_3CN{\cdot}2(CH_3)_2CO$ showing positions of anions and solvents.

Table 1. Crystal and Data Collection Parameters for $NiTF_4TMAP(CF_3SO_3)_4{\cdot}2CH_3CN{\cdot}2(CH_3)_2CO$

formula	$C_{70}H_{44}F_{28}N_{10}NiO_{14}S_4$
MW	1968.1
space group	$P\bar{1}$
a, Å	14.090(3)
b, Å	15.725(3)
c, Å	19.554(4)
α, deg	78.43(3)
β, deg	77.26(3)
γ, deg	83.14(3)
V, Å³	4127
Z	2
T, °C	−120
radiation	Cu Kα (graphite monochromator)
2*θ* range, deg	2.0−102.5
scan type	*ω*
scan speed, deg/min	8.0−60.0
no. of reflcns collected	9387
no. of unique reflcns used in least-square fit	7376 with $F_o > 4\sigma(F_o)$
R on F_o for data with $F_o > 4\sigma(F_o)$	0.0759
R_w on F_o for data with $F_o > 4\sigma(F_o)$	0.0791

$(CF_3SO_3)_4{\cdot}2CH_3CN{\cdot}2(CH_3)_2CO$ was solved by direct methods[48] which showed two porphyrin molecules in the unit cell. Calculated hydrogen positions were entered and constrained to riding motions with fixed isotropic *U*.

Titration Studies in Non-Aqueous Solution. Spectrophotometric measurements were made by titration of solutions of porphyrins (5×10^{-6} to 2×10^{-5} M) with ligand in 1.00 cm path length quartz cuvettes at 25.0 °C. Binding constants were calculated using nonlinear curve fitting routines in the program KaleidaGraph 3.0 (Synergy Software, Reading PA). In all cases where two binding constants are reported, attempted fits to single step binding of one or two ligands were unsatisfactory as judged by plots of calculated and measured absorbance vs log([ligand]). Quoted errors are derived from multiple titrations and analysis at different wavelengths.

Titration Studies in Aqueous Solution. Aliquots of acetone or acetonitrile were titrated into a solution of $Ni(TF_4TMAP)Cl_4$ in H_2O, and a visible spectrum was recorded after each addition. Spectrophotometric measurements of interactions with organic solutes were performed by titration of aqueous solutions of $Ni(TF_4TMAP)(CF_3SO_3)_4$ or $Ni(TF_4TMAP)Cl_4$ with 4-morpholineethanesulfonic acid (MES), 4-(2-hydroxyethyl)-1-piperazineethanesulfonic acid (HEPES), 3-phenylpropanoic acid , terephthalic acid, and phenylacetic acid after adjustment to specified pH values. Measurements for disodium 2,6-naphthalene sulfonate, sodium 4-toluenesulfonate, tetraethylammonium perfluoro-1-octanesulfonate, 1-naphthol, and acetophenone were obtained without adjusting solution pH.

Results

Crystal Structure. The crystal structure of $Ni(TF_4TMAP)(CF_3SO_3)_4{\cdot}2CH_3CN{\cdot}2(CH_3)_2CO$ is shown in Figures 1 and 2, and Figure 3 shows the relative positions of the atoms in the porphyrin skeleton and their displacements from the rms plane of the porphyrin ring N atoms. Table 2 shows the equilibrium atom positions and isotropic thermal parameters, and Table 3 shows selected bond distances and angles in the porphyrin cation. There is no evidence for axial coordination of the Ni(II) by either $CF_3SO_3^-$ or solvent. The overall structure is typical of four-coordinate square planar Ni(II) porphyrins, in which the porphyrin ring becomes distorted to accommodate the small four-coordinate Ni(II) ion.[49−51] The average Ni−N distance is 1.928 which is in the middle of the range of measured Ni(II) porphyrin Ni−N distances (1.960−1.902 Å), and this leads to a mild distortion of the porphyrin ring. This is demonstrated by the value of the trans N−Ni−N angle (177.9 and 178.9°) which indicates little doming of the porphyrin, although the dihedral $C\alpha{-}N{-}N_{trans}{-}C\alpha$ angles (26.4, 26.1, 26.7, and 19.8°) show that there is significant buckling across the porphyrin ring.[50−52] The only other structure of a water-soluble nickel porphyrin is that for $Ni^{II}T(4\text{-}NMePyP)(ClO_4)_2(Im)_2{\cdot}2(CH_3)_2CO$, which is six-coordinate and high spin.[53] This complex has electron population in the antibonding $d_{x^2-y^2}$ orbital, and so although the nickel also lies in the porphyrin plane, the effective radius of the Ni(II) has increased and the Ni−N distances increase to an average of 2.038 Å. This porphyrin therefore does not show the distortions seen for the square-planar Ni complexes.

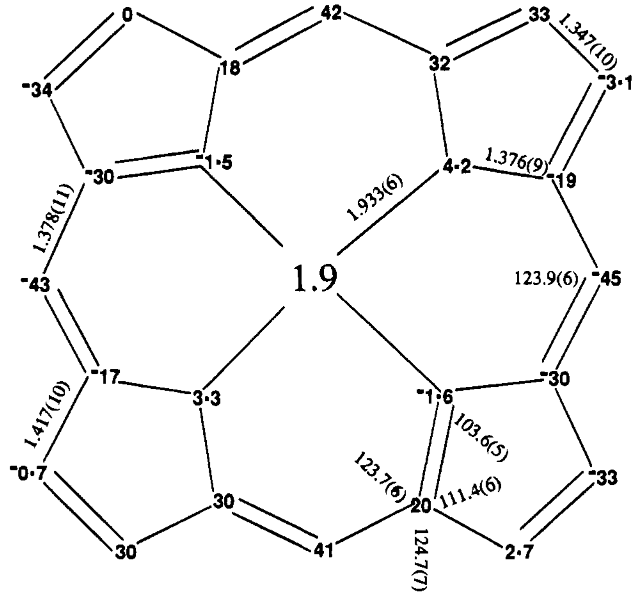

Figure 3. Diagram showing the deviations of the porphyrin core atoms from the rms plane defined by the four central nitrogen atoms. Displacements are given in pm (0.01 Å). Selected bond distances and bond angles are also shown.

There is no obvious steric effect on the porphyrin ring due to the fluorine substituents, in agreement with the crystal structure of $Co(TF_4DMAP)$ reported by Kadish and co-workers.[54] The dihedral angles between the porphyrin and the phenyl

---

(49) Meyer, E. F. *Acta Crystallogr.* **1972**, *B28*, 2162.

(50) Shelnutt, J. A.; Medforth, C. J.; Berber, M. D.; Barkigia, K. M.; Smith, K. M. *J. Am. Chem. Soc.* **1991**, *113*, 4077.

(51) Barkigia, K. M.; Renner, M. W.; Furenlid, L. R.; Medforth, C. J.; Smith, K. M.; Fajer, J. *J. Am. Chem. Soc.* **1993**, *115*, 3627.

(52) Sparks, L. D.; Anderson, K. K.; Medforth, C. J.; Smith, K. M.; Shelnutt, J. A. *Inorg. Chem.* **1994**, *33*, 2297.

(53) Kirner, J. F.; Garofalo, J. J.; Scheidt, W. R. *Inorg. Nucl. Chem. Lett.* **1975**, *11*, 107.

(54) Kadish, K. M.; Araullo-McAdams, C.; Han, B. C.; Franzen, M. M. *J. Am. Chem. Soc.* **1990**, *112*, 8364.

Table 2. Atomic Coordinates ($\times 10^5$) and Equivalent Isotropic Displacement Coefficients ($Å^2 \times 10^4$)

	x	*y*	*z*	*U*(eq)[a]		*x*	*y*	*z*	*U*(eq)[a]
Ni(1)	3182(9)	20153(8)	12136(6)	169(4)	C(12)	23851(55)	2094(48)	20898(39)	258(9)
S(1)	−14622(18)	72641(16)	−50646(12)	399(7)	C(13)	25587(55)	155(47)	14334(40)	265(9)
S(2)	−43840(18)	54434(15)	−17221(12)	373(7)	C(14)	19401(53)	6191(45)	10367(38)	206(9)
S(3)	71261(17)	37161(14)	46801(11)	320(6)	C(15)	19956(55)	6986(47)	3145(38)	234(9)
S(4)	52650(23)	4545(17)	67633(13)	592(7)	C(16)	15000(55)	13842(47)	−785(38)	239(9)
F(1)	−24869(33)	46323(27)	23348(24)	347(8)	C(17)	16896(60)	15984(50)	−8328(39)	332(9)
F(2)	−41682(33)	50253(27)	31105(24)	373(9)	C(18)	11263(59)	23099(49)	−10119(40)	316(9)
F(3)	−47388(31)	20127(28)	36967(23)	347(8)	C(19)	5566(54)	25341(45)	−3719(36)	197(9)
F(4)	−30558(31)	16651(26)	29116(22)	290(8)	C(20)	−1940(54)	31653(45)	−3309(36)	196(9)
F(5)	4065(33)	−1343(29)	38150(23)	371(9)	C(21)	−27002(53)	31402(46)	25823(37)	191(9)
F(6)	10510(34)	−7105(28)	49835(23)	374(8)	C(22)	−30470(54)	39750(48)	26592(39)	241(9)
F(7)	34985(33)	13066(29)	41893(23)	360(8)	C(23)	−39500(56)	41741(48)	30945(39)	257(9)
F(8)	28067(33)	18742(27)	30520(22)	316(8)	C(24)	−45431(52)	35354(48)	34513(37)	209(9)
F(9)	14757(36)	−9116(31)	1552(29)	571(9)	C(25)	−42189(54)	27003(47)	33683(37)	223(9)
F(10)	26652(38)	−20473(31)	−4773(29)	589(9)	C(26)	−33227(53)	24981(45)	29550(37)	201(9)
F(11)	51927(35)	−1327(30)	−9656(29)	519(9)	C(27)	15757(52)	9070(44)	33848(37)	182(9)
F(12)	39863(36)	9732(31)	−3351(29)	543(9)	C(28)	11673(53)	2426(49)	39083(41)	252(9)
F(13)	−11620(37)	26376(28)	−12831(24)	417(9)	C(29)	15137(54)	−739(46)	45229(38)	215(9)
F(14)	−15005(36)	35634(28)	−24592(24)	425(9)	C(30)	23155(52)	2499(46)	46499(37)	202(9)
F(15)	460(35)	58787(27)	−20224(24)	377(9)	C(31)	27275(52)	9215(47)	41322(40)	221(9)
F(16)	3539(36)	48985(28)	−8293(23)	407(9)	C(32)	23592(53)	12211(45)	35187(37)	196(9)
F(17)	−4106(50)	69445(45)	−62634(31)	972(9)	C(33)	26769(57)	698(46)	−642(38)	244(9)
F(18)	836(51)	79404(44)	−58244(40)	1109(9)	C(34)	23875(58)	−7044(50)	−1266(42)	313(9)
F(19)	3073(43)	65753(43)	−53905(35)	911(9)	C(35)	30296(61)	−13013(48)	−4623(43)	341(9)
F(20)	−29279(43)	46471(45)	−11851(32)	932(9)	C(36)	39919(55)	−11496(46)	−7606(38)	225(9)
F(21)	−40466(40)	52068(37)	−4390(26)	615(9)	C(37)	42883(54)	−3715(48)	−7090(40)	260(9)
F(22)	−42707(54)	40539(35)	−7753(30)	925(9)	C(38)	36460(58)	2174(48)	−3687(41)	292(9)
F(23)	62691(46)	30717(44)	59676(29)	885(9)	C(39)	−4000(53)	37381(47)	−10116(38)	220(9)
F(24)	74407(46)	38453(38)	59253(31)	804(9)	C(40)	−8646(55)	34398(47)	−14616(39)	241(9)
F(25)	77507(45)	25627(36)	56863(30)	740(9)	C(41)	−10402(54)	39376(46)	−20823(37)	212(9)
F(26)	44192(59)	19737(17)	68691(46)	1497(10)	C(42)	−7672(51)	47816(46)	−22952(36)	178(9)
F(27)	41183(65)	10434(55)	78134(10)	1539(10)	C(43)	−2886(55)	50815(46)	−18620(39)	240(9)
F(28)	34616(32)	10299(59)	69607(45)	1558(10)	C(44)	−1165(54)	45572(48)	−12274(39)	240(9)
O(1)	52395(52)	5570(51)	60355(18)	817(9)	C(45)	−57825(61)	46097(55)	40038(47)	440(9)
O(2)	60962(42)	7889(51)	68660(46)	1092(9)	C(46)	−63011(56)	33957(53)	36511(42)	334(9)
O(3)	51287(78)	−3938(32)	71489(52)	1716(10)	C(47)	−54862(62)	31673(60)	46809(44)	479(9)
O(4)	80626(47)	40097(43)	43843(38)	689(9)	C(48)	19156(58)	−179(50)	59517(38)	304(9)
O(5)	69239(41)	29641(34)	44387(28)	375(9)	C(49)	29742(61)	−10987(50)	53006(42)	357(9)
O(6)	63380(43)	43885(36)	47176(30)	428(9)	C(50)	35876(58)	2384(53)	53939(44)	367(9)
O(7)	−39475(50)	62552(36)	−18506(31)	555(9)	C(51)	46811(68)	−26684(51)	−5510(45)	478(9)
O(8)	−40441(50)	49462(37)	−22809(30)	537(9)	C(52)	56857(62)	−16394(55)	−13759(47)	458(9)
O(9)	−54203(47)	55023(48)	−14507(38)	751(9)	C(53)	42561(62)	−2008(52)	−17127(42)	381(9)
O(10)	−12390(50)	74441(44)	−44437(33)	663(9)	C(54)	695(57)	55765(53)	−34544(41)	358(9)
O(11)	−17900(49)	63776(40)	−49563(35)	622(9)	C(55)	−14856(60)	49963(50)	−33978(41)	334(9)
O(12)	−20558(46)	79030(38)	−54388(32)	547(9)	C(56)	−14957(59)	62042(50)	−27978(44)	352(9)
N(1)	−7389(42)	28426(35)	9711(29)	152(9)	C(57)	−3034(71)	71849(62)	−56871(51)	630(9)
N(2)	−1553(41)	20839(36)	22074(30)	158(9)	C(58)	−38819(64)	48213(55)	−9961(44)	453(9)
N(3)	13385(44)	11581(37)	14667(30)	206(9)	C(59)	71718(64)	32783(58)	56125(48)	492(9)
N(4)	8005(44)	19684(36)	2229(31)	195(9)	C(60)	42866(22)	11502(16)	71172(9)	955(10)
N(5)	−55080(46)	36782(42)	39341(32)	305(9)	N(9)	13869(61)	37316(53)	74239(42)	672(9)
N(6)	26940(45)	−1444(39)	53088(32)	257(9)	C(61)	20245(67)	37126(55)	69587(47)	462(9)
N(7)	46410(49)	−18518(39)	−10860(32)	300(9)	C(62)	28357(64)	36883(58)	63430(46)	498(9)
N(8)	−9183(45)	53700(39)	−29801(32)	260(9)	N(10)	82438(65)	5043(63)	17149(57)	1139(10)
C(1)	−8491(53)	32876(44)	3115(39)	192(9)	C(63)	89225(69)	459(68)	17752(68)	1028(10)
C(2)	−17532(54)	38113(46)	3500(38)	226(9)	C(64)	97413(71)	−6383(67)	19940(69)	1125(10)
C(3)	−22254(53)	36763(46)	10249(37)	203(9)	O(13)	61312(61)	19053(46)	90178(36)	930(9)
C(4)	−15772(50)	31007(43)	14185(37)	153(9)	C(65)	66095(86)	24558(81)	76656(47)	1244(10)
C(5)	−17326(50)	28825(44)	21515(36)	157(9)	C(66)	60155(67)	22722(58)	84463(37)	653(9)
C(6)	−10361(52)	24572(44)	25193(36)	170(9)	C(67)	50515(74)	27391(87)	82390(81)	1682(10)
C(7)	−10943(52)	24019(45)	32643(37)	196(9)	O(14)	27999(77)	38405(69)	−6875(47)	1704(10)
C(8)	−2422(54)	20101(46)	34151(36)	202(9)	C(68)	19419(77)	36516(73)	6883(51)	995(10)
C(9)	3258(53)	17752(44)	27705(36)	167(9)	C(69)	25453(83)	35683(68)	−698(47)	1242(10)
C(10)	11814(51)	12385(45)	27227(37)	173(9)	C(70)	30985(83)	26680(66)	1459(67)	1072(10)
C(11)	16271(51)	9077(45)	21088(37)	178(9)					

[a] Equivalent isotropic *U* defined as one-third of the trace of the orthogonalized $\mathbf{U}_{ij}$ tensor.

substituents are 69, 75, 79, and 89°, which are within the range found for H-substituted tetraphenylporphyrins (60−90°).[55] A comparison of selected distances in this porphyrin and in the cobalt complexes of its precursors Co(TF$_4$DMAP) and Co(TF$_5$PP)[54] is given in Table 4. The only significant change in the phenyl substituents are the lengthening of the C−N(ammonium) bond lengths, in accord with comparisons of dialkylanilines and their trialkylated anilinium salts.[56,57] The porphyrin cores are not compared because the smaller Ni^{II} ($r = 0.63$ Å) causes large distortions in the porphyrin ring compared to the larger Co^{II} (0.7−0.9 Å).[58]

---

(55) Hoard, J. L. In *Porphyrins and Metalloporphyrins*; Smith, K. M., Ed.; Elsevier: Amsterdam, 1975; p 317.

Table 3. Selected Bond Distances (Å) and Bond Angles in the NiTF$_4$MAP^{4+} Cation

Ni(1)−N(1)	1.933(6)	Ni(1)−N(2)	1.931(6)
Ni(1)−N(3)	1.927(6)	Ni(1)−N(4)	1.920(6)
N(1)−C(1)	1.370(9)	N(1)−C(4)	1.378(8)
N(2)−C(6)	1.376(9)	N(2)−C(9)	1.394(10)
N(3)−C(11)	1.373(10)	N(3)−C(14)	1.394(9)
N(4)−C(16)	1.381(9)	N(4)−C(19)	1.397(9)
C(1)−C(2)	1.428(10)	C(1)−C(20)	1.418(10)
C(2)−C(3)	1.328(9)	C(3)−C(4)	1.442(10)
C(4)−C(5)	1.379(10)	C(5)−C(6)	1.374(10)
C(6)−C(7)	1.426(10)	C(7)−C(8)	1.347(10)
C(8)−C(9)	1.427(10)	C(9)−C(10)	1.383(10)
C(10)−C(11)	1.395(10)	C(11)−C(12)	1.438(10)
C(12)−C(13)	1.342(11)	C(13)−C(14)	1.438(10)
C(14)−C(15)	1.378(11)	C(15)−C(16)	1.402(10)
C(16)−C(17)	1.417(10)	C(17)−C(18)	1.326(11)
C(18)−C(19)	1.415(10)	C(19)−C(20)	1.362(10)

N(1)−Ni(1)−N(2)	89.7(2)	N(1)−Ni(1)−N(3)	177.9(3)
N(2)−Ni(1)−N(3)	89.8(2)	N(1)−Ni(1)−N(4)	90.1(2)
N(2)−Ni(1)−N(4)	178.9(3)	N(3)−Ni(1)−N(4)	90.4(2)
Ni(1)−N(1)−C(1)	128.3(4)	Ni(1)−N(1)−C(4)	128.1(4)
Ni(1)−N(2)−C(6)	128.0(5)	Ni(1)−N(2)−C(9)	127.7(4)
Ni(1)−N(3)−C(11)	129.1(5)	Ni(1)−N(3)−C(14)	127.4(5)
Ni(1)−N(4)−C(16)	128.6(5)	Ni(1)−N(4)−C(19)	128.6(5)
N(1)−C(1)−C(2)	111.4(6)	N(1)−C(1)−C(20)	123.7(6)
N(1)−C(4)−C(5)	123.6(6)	N(1)−C(4)−C(3)	111.3(6)
N(2)−C(6)−C(5)	124.3(6)	N(2)−C(6)−C(7)	110.8(6)
N(2)−C(9)−C(8)	110.5(6)	N(2)−C(9)−C(10)	124.3(6)
N(3)−C(11)−C(10)	124.0(6)	N(3)−C(11)−C(12)	111.9(6)
N(3)−C(14)−C(13)	111.0(7)	N(3)−C(14)−C(15)	124.7(6)
N(4)−C(16)−C(15)	124.1(6)	N(4)−C(16)−C(17)	111.3(6)
N(4)−C(19)−C(18)	111.2(6)	N(4)−C(19)−C(20)	123.4(6)
C(1)−C(2)−C(3)	107.6(6)	C(1)−N(1)−C(4)	103.6(5)
C(1)−C(20)−C(19)	123.9(6)	C(2)−C(1)−C(20)	124.7(7)
C(2)−C(3)−C(4)	106.1(6)	C(3)−C(4)−C(5)	124.9(6)
C(4)−C(5)−C(6)	123.9(6)	C(5)−C(6)−C(7)	124.7(6)
C(6)−N(2)−C(9)	104.3(6)	C(6)−C(7)−C(8)	107.4(6)
C(7)−C(8)−C(9)	106.8(7)	C(8)−C(9)−C(10)	124.9(7)
C(9)−C(10)−C(11)	123.0(7)	C(10)−C(11)−C(12)	123.9(7)
C(11)−N(3)−C(14)	103.5(6)	C(11)−C(12)−C(13)	106.7(7)
C(12)−C(13)−C(14)	106.9(6)	C(13)−C(14)−C(15)	124.1(7)
C(14)−C(15)−C(16)	122.7(7)	C(15)−C(16)−C(17)	124.6(7)
C(16)−N(4)−C(19)	102.8(5)	C(16)−C(17)−C(18)	107.6(7)
C(17)−C(18)−C(19)	107.1(6)	C(18)−C(19)−C(20)	125.1(7)

The anions are located in channels formed by the porphyrins. There is no disorder of the $CF_3SO_3^-$ ions or the solvent, in contrast to previous water-soluble porphyrin crystal structures.[53,59] This can be attributed both to the use of the lower-symmetry $CF_3SO_3^-$ anion (previous studies used ClO_4^- and I^-) and to the use of non-aqueous media for the crystallization. The Ni−Ni distance between porphyrins is 8.88 Å, indicating no tendency for $\pi-\pi$ interactions.

Non-Aqueous Solutions. The absorption spectra of Ni(TF$_4$TMAP)$^{4+}$ is typical for nickel metalloporphyrins, with the intense Soret band at 399 nm and the weaker Q transitions at 523 and 556 nm. There was no evidence for dimerization of the Ni^{II} porphyrins under any conditions.[60] In the presence of nitrogenous bases such as pyridine, 1-methylimidazole, and *n*-butylamine, a new Soret band appeared at 425−430 nm. As the concentration of the base increased, the Soret band at 399 nm decreased in intensity while the ca. 427 nm band increased. Concomitant with this, the Q band at 523 nm diminished and the Q band at 556 nm slightly blue-shifted to 554 nm and increased in absorbance, Figure 4a and Table 5. Addition of tri-n-butylphosphine to a solution of Ni(TF$_4$TMAP)$^{4+}$ caused the Soret band to red-shift to 409 nm and decrease in absorbance. A shoulder at 450 nm grew as the concentration of tri-*n*-butylphosphine increased, and only one Q band was observed at 554 nm, Figure 4b. The absorbance spectrum of Ni(TF$_4$TMAP)$^{4+}$ was only slightly affected by the presence of thiophenol (0.13 M). The spectrum of Ni(TF$_4$TMAP)$^{4+}$ in DMSO shows peaks corresponding to both the square planar and axially ligated nickel, and this is also reflected in the ^{1}H NMR spectrum which shows a β-pyrrole peak at 42.8 ppm,

Table 4. Comparison of Bond Lengths in the Fluorinated Phenyl Substituents of Cobalt 5,10,15,20-Tetrakis(pentafluorophenyl)porphyrin (CoTF$_5$PP), Cobalt 5,10,15,20-Tetrakis(2,3,5,6-tetrafluoro-*N*,*N*-dimethyl-4-anilinyl)porphyrin (CoTF$_4$DMAP), and Nickel 5,10,15,20-Tetrakis(2,3,5,6-tetrafluoro-*N*,*N*,*N*-trimethyl-4-aniliniumyl)porphyrin (NiTF$_4$TMAP^{4+})

bonds averaged[a]	CoTF$_5$PP[b]	CoTF$_4$DMAP[b]	NiTF$_4$TMAP^{4+}
$C_{Ph}-F$	1.333(15)	1.346(15)	1.332(15)
$C_{por}-C_{Ph}$	1.495(9)	1.491(13)	1.497(13)
$C_{Ph}-N_{am}$		1.38(2)	1.499(10)
$N_{am}-C_{Me}$		1.39(2)	1.508(12)

[a] All bond lengths are in Å. C_{Ph} = C on phenyl ring; C_{Por} = C on porphyrin ring; N_{Am} = aniline (or anilinium) nitrogen; C_{Me} = methyl carbons. [b] Taken from ref 53.

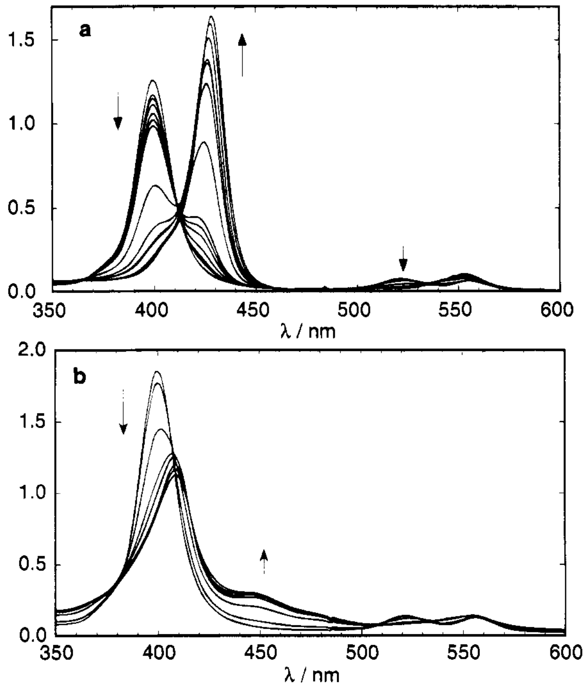

Figure 4. Titration of NiTF$_4$TMAP^{4+} in acetonitrile with (a) pyridine and (b) tris(*n*-butyl)phosphine at 25.0 °C: (a) [pyridine] = 0.0, 1.0, 2.0, 4.0, 6.0, 8.0, 10, 30, 60, and 90 mM and 0.10, 0.50, 3.0, and 6.0 M); (b) [PBu$_3$] = 0.0, 0.10, 1.0, 5.0, 10, 30, 60, and 90 mM.

Table 5. Absorbance Maxima for NiTF$_4$TMAP^{4+} Species

solvent	species	coord no.	λ_{max}, nm
acetonitrile	NiTF$_4$TMAP^{4+}	4	399, 523, 556
	NiTF$_4$TMAP(1-MeIm)$^{4+}$	5	424, 556
	NiTF$_4$TMAP(1-MeIm)$_2$$^{4+}$	6	430, 554
	NiTF$_4$TMAP(py)$_2$$^{4+}$	6	427, 554
	NiTF$_4$TMAP(PBu$_3$)$^{4+}$	5	409
	NiTF$_4$TMAP(PBu$_3$)$_2$$^{4+}$	6	409, 450 (sh), 554
H_2O	NiTF$_4$TMAP^{4+}	4	400, 523, 557
	NiTF$_4$TMAP(H_2O)$_2$$^{4+}$	6	421, 552

---

(56) Sorriso, S. In *The chemistry of amino, nitroso and nitro compounds and their derivatives Part 1*; Patai, S., Ed.; John Wiley & Sons Ltd.: New York, 1982; p 1.

(57) Krug, V. V.; Muller, U. *Acta Crystallogr.* **1989**, *C45*, 2022.

(58) Shannon, R. D. *Acta Crystallogr.* **1976**, *A32*, 751.

(59) Ivanca, M. A.; Lappin, A. G.; Scheidt, W. R. *Inorg. Chem.* **1991**, *30*, 711.

(60) Kadish, K. M.; Sazou, D.; Liu, Y. M.; Saoiabi, A.; Ferhat, M.; Guilard, R. *Inorg. Chem.* **1988**, *27*, 686.

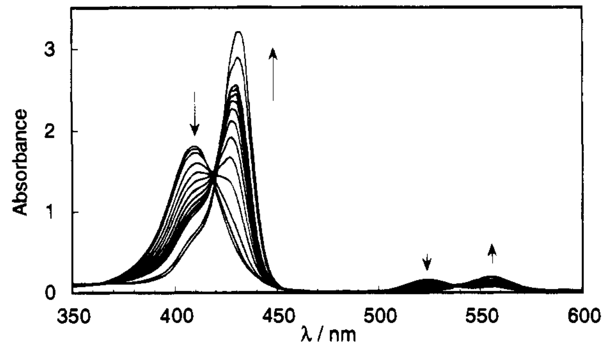

Figure 5. Titration of NiTF$_4$DMAF in acetone with pyridine. [pyridine] = 0.0, 0.050, 0.10, 0.20, 0.30, 0.40, 0.50, 0.60, 0.70, 0.80, 0.90, 1.0, 3.0, and 6.0 M.

Table 6. Binding Constants for Ligation to Ni(TF$_4$DMAP) and Ni(TF$_4$TMAP)$^{4+}$

	ligand	solvent	K_1	K_2	K_1K_2
Ni(TF$_4$DMAP)	MeIm	DMF	7 ± 1	2.5 ± 0.5	
	MeIm	acetone	10 ± 2	3 ± 1	
	Py	DMF			~8
	Py	CH$_2$Cl$_2$			~4
Ni(TF$_4$TMAP)$^{4+}$	MeIm	MeCN	550 ± 50	110 ± 20	
	Py	MeCN	33 ± 5	50 ± 10	
	PhSH	MeCN			small
	PBu$_3$	MeCN	1200 ± 400	30 ± 10	
	DMSO	DMSO	~0.05		

intermediate between that in MeCN (9.24 ppm) and that in the presence of a strong axial base such as 1-methylimidazole (53.7 ppm). Results for ligand binding calculated from non-linear least-squares fit of the spectrophotometric titration data for all these ligands are given in Table 6.

Titrations of Ni(TF$_4$DMAP) in acetone, DMF, or CH$_2$Cl$_2$ with 1-methylimidazole or pyridine all gave similar results regardless of the base or solvent system employed, Table 6. The absorption spectrum of Ni(TF$_4$DMAP) has the Soret band near 412 nm and two Q bands at 524 and 557 nm. In the presence of nitrogenous bases such as 1-methylimidazole or pyridine the absorbance intensity of the Soret band near 412 nm is reduced and a new Soret is generated at 430 nm. The Q band at 524 nm gradually diminishes as the concentration of the base increases while the Q band at 557 remains unchanged, Figure 5. The spectrum of Ni(TF$_4$DMAP) in dimethyl sulfoxide is identical to that in the other organic solvents, showing that little or no coordination by DMSO occurs.

Aqueous Chemistry of H$_2$T(4-NMePyP)$^{4+}$. The cationic porphyrin H$_2$T(4-NMePyP)$^{4+}$ has been much studied and is frequently used as a basis for comparison with the behavior of other porphyrins. It has therefore been of concern that several groups have suggested that H$_2$T(4-NMePyP)$^{4+}$ is not well characterized in solution and in fact exists as a dimer under most conditions.[15,61-65] These suggestions have been made on the basis of deviations from Beer's law,[61] changes in the fluorescence spectrum at low concentrations,[61-64] and variations in time-dependent fluorescence spectroscopy[65] and resonance raman spectra.[15] These studies suggested that dimerization of porphyrins might not be detectable using UV–visible spectroscopy or NMR. This would be of serious concern since many porphyrin solution studies rely on these techniques. Therefore we decided to reexamine the H$_2$T(4-NMePyP)$^{4+}$ system to confirm the validity of conclusions made using NMR and UV–visible data. Remeasurement of the steady-state fluorescence and UV–visible spectra in our laboratory suggests that the previous reports were probably due to artifacts associated with the low concentrations of porphyrin used. Thus, at [porphyrin] < 10^{-7} M, leaving solutions in quartz cuvettes or bubbling N$_2$ through a quartz cuvette using a disposable pasteur pipet caused significant decreases in the fluorescence signal, suggesting considerable adsorption. In our hands Beer's law plots were linear to the lowest concentrations used (5 × 10^{-7} M) when 1.00 cm plastic cuvettes were used and measurements were made shortly after dilution. Of even more significance were analyses for the perturbation of chemical equilibria by dimerizations. Previous authors have stated that addition of organic solvent or an increase in temperature caused the monomerization of the reportedly dimeric porphyrin.[62] We find that increasing the temperature to 50 °C or addition of 20% methanol to H$_2$T(4-NMePyP)$^{4+}$ solutions causes exactly the same perturbation of the fluorescence spectrum at 1 × 10^{-5} M and 5 × 10^{-7} M porphyrin, Figure 6, requiring that any dimerization has a dimerization constant less than 2 × 10^4 M^{-1}. Also, the spectra of 5 × 10^{-7} to 5 × 10^{-5} M porphyrin in 0.1 M HCl follow Beer's law, Figure 7. Since this acid concentration corresponds to partial protonation of the porphyrin at an ionic strength of 0.1 M, and assuming that the protonated porphyrin does not dimerize,[66] this also places an upper limit on the dimerization constant of 2 × 10^4 M^{-1}. This value overlaps with previous Beer's law and NMR results reporting that the state of aggregation is invariant between 10^{-5} and 10^{-3} M[25,67,68] and shows that H$_2$T(4-NMePyP)$^{4+}$ is monomeric at all concentrations below 10^{-3} M. An attempt to generate a dimer using the induced association with BPh$_4^-$ reported by Armitage and coworkers for other cationic dyes[69] appeared to cause nonspecific aggregation (red-shift and decrease in Soret intensity) followed

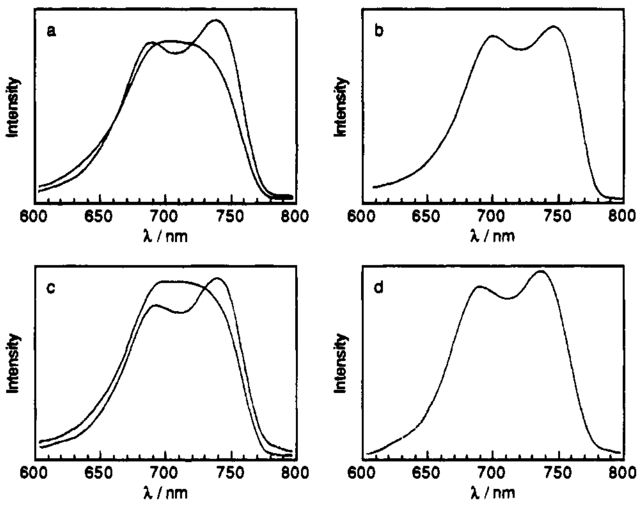

Figure 6. Fluorescence measurements of H$_2$T4-NMePyP^{4+} (arbitrary intensity scale): (a) 1 × 10^{-5} H$_2$T4-NMePyP^{4+} with and without 20% methanol at 25 °C; (b) 1 × 10^{-5} M H$_2$T4-NMePyP^{4+} at 50 °C; (c) 5 × 10^{-7} M H$_2$T4-NMePyP^{4+} with and without 20% methanol at 25 °C; (d) 5 × 10^{-7} M H$_2$T4-NMePyP^{4+} at 50 °C.

---

(61) Brookfield, R. L.; Ellul, H.; Harriman, A. *J. Photochem.* **1985**, *31*, 97.

(62) Kano, K.; Miyake, T.; Uomoto, K.; Sato, T.; Ogawa, T.; Hahimoto, S. *Chem. Lett.* **1983**, 1867.

(63) Kano, K.; Nakajima, T.; Takei, M.; Hashimoto, S. *Bull. Chem. Soc. Jpn* **1987**, *60*, 1281.

(64) Kano, K.; Takei, M.; Hashimoto, S. *J. Phys. Chem.* **1990**, *94*, 2181.

(65) Kemnitz, K.; Sakaguchi, T. *Chem. Phys. Lett.* **1992**, *196*, 497.

(66) Harriman, A.; Richoux, M.-C. *J. Photochem.* **1984**, *27*, 205.

(67) Foster, N. *J. Magn. Reson.* **1984**, *56*, 140.

(68) Pasternack, R. F.; Huber, P. R.; Boyd, P.; Engasser, G.; Francesconi, L.; Gibbs, E.; Fasella, P.; Cerio Venturo, G.; deC. Hinds, L. *J. Am. Chem. Soc.* **1972**, *94*, 4511.

(69) Armitage, B.; Retterer, J.; O'Brien, D. F. *J. Am. Chem. Soc.* **1993**, *115*, 10786.

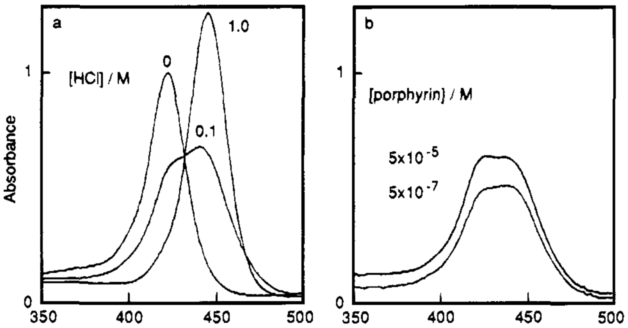

Figure 7. Absorbance spectra of $H_xT4\text{-}NMePyP^{(2+n)+}$: (a) 5.0 × 10^{-6} M $H_xT4\text{-}NMePyP^{(2+n)+}$ at different concentrations of hydrochloric acid (1.00 cm cell; no control of ionic strength); (b) 5.0 × 10^{-5} M $H_xT4\text{-}NMePyP^{(2+n)+}$ (0.100 cm cell) and 5.0 × 10^{-7} M $H_xT4\text{-}NMePyP^{(2+n)+}$ (1.00 cm cell × 10) in 0.10 M HCl.

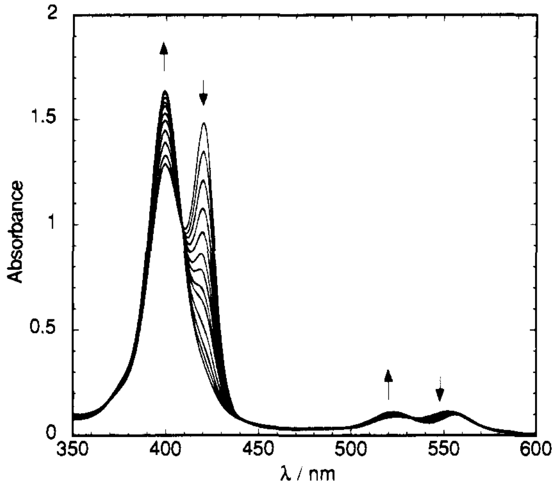

Figure 8. Titration of an aqueous solution of $NiTF_4TMAP^{4+}$ with acetonitrile at 25.0 °C. [MeCN] = 0.0, 0.048, 0.14, 0.24, 0.32, 0.42, 0.52, 0.62, 0.69, 0.91, 1.24, 1.53, and 1.74 M.

by precipitation, even at substoichiometric levels (<5 × 10^{-5} M). Our conclusions about the monomeric nature of this porphyrin are in accord with the findings of previous researchers,[25,67,70] and leave little doubt that $H_2T(4\text{-}NMePy)P^{4+}$ is monomeric in aqueous solutions at concentrations below 10^{-3} M.

Aqueous Chemistry of $Ni(TF_4TMAP)^{4+}$. The room temperature absorption spectrum of an aqueous solution of $Ni(TF_4TMAP)Cl_4$ shows a Soret region composed of two bands at 400 and 420 nm, along with two Q-bands near 523 and 552 nm. At low temperature (~5 °C) the 421 and 552 nm bands increased at the expense of the 400 and 523 nm bands. When the temperature of the $Ni(TF_4TMAP)Cl_4$ solution was raised to 70 °C, the band at 400 nm was predominant while the 421 nm band was suppressed, and the Q-bands had comparable intensities (λ_{max} 523 and 557 nm). The addition of acetone or acetonitrile also promoted the 400 nm band and decreased the 421 nm band. Isosbestic points were observed at 410 and 433 nm, Figure 8. On the basis of previous studies[8,24,46] and our studies in non-aqueous solvents, we assign the 400 nm peak to four-coordinate nickel and the 421 nm band to the six-coordinate bis(aquo) form, Table 5.

Comparison of the Behavior of $NiT(4\text{-}NMePyP)^{4+}$ and $Ni(TF_4TMAP)^{4+}$. An earlier study of the aqueous chemistry of $NiT(4\text{-}NMePyP)^{4+}$ reported that the porphyrin was an equilibrium mixture of four and six-coordinate nickel in aqueous solution, but that addition of organic solvents such as acetone caused the displacement of the equilibrium toward the four-coordinate form, Figure 9.[46] As reported above, $Ni(TF_4TMAP)^{4+}$ behaves in a similar fashion. However, the equilibrium in pure water lies more heavily toward the six-coordinate form than for $NiT(4\text{-}NMePyP)^{4+}$, Figure 9, presumably because the Ni center is more electron-deficient. The equilibrium in water was estimated both from the Soret bands (using the high and low temperature limiting spectra to obtain values for the four- and six-coordinated species, or using the values for the six-coordinated species in organic solvents) and from NMR experiments, again using the value obtained in the presence of an excess of ligand in organic solvents as the high spin limit. The analysis was made only in terms of four- and six-coordinate species, even though some bases clearly form a five-coordinate intermediate species. This was rationalized both because the data did not support significant concentrations of a five-coordinate species and because the coordination of most other weak axial bases appears to be concerted (i.e. $K_2 > K_1$, vide infra). Addition of organic solvent causes a more rapid decrease in the amount of the six-coordinate species for $Ni(TF_4TMAP)^{4+}$ than for $NiT(4\text{-}NMePyP)^{4+}$, due to the increased hydrophobic nature of the fluorinated porphyrin.

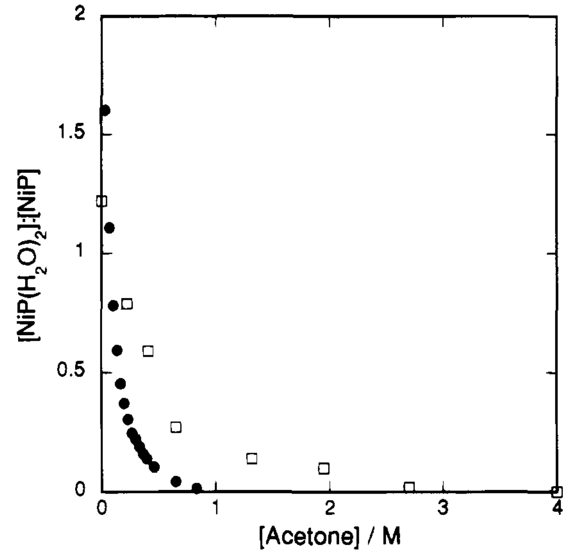

Figure 9. Plot of the ratio of the amount of Ni^{II} porphyrin present as the six-coordinate diaquo form to the amount present as the four-coordinate form for $NiTF_4TMAP^{4+}$ (●) and $NiT4\text{-}NMePyP^{4+}$ (□) as aqueous solutions are titrated with acetone. Data for $NiT4\text{-}NMePyP^{4+}$ are taken from ref 45.

Interaction of $Ni(TF_4TMAP)^{4+}$ with Organic Substrates. The hydrophobic character of the porphyrin was probed by adding organic substrates such as 2,6-naphthalenedisulfonate, MES, HEPES, 4-toluenesulfonate, perfluoro-1-octanesulfonate, 3-phenylpropanoic acid, phenylacetic acid, terephthalic acid, potassium hydrogen phthalate, 1,3-benzenedisulfonic acid, 1-naphthol, and acetophenone into aqueous solutions of $Ni(TF_4TMAP)Cl_4$, Table 7. Aromatic sulfonates such as 2,6-naphthalenedisulfonate, 1,3-benzenedisulfonic acid, and 4-toluenesulfonate affected the visible spectrum of the aqueous solution of $Ni(TF_4TMAP)Cl_4$ at the submillimolar level at all pH's, causing the 400 nm band to predominate while the 420 nm band was suppressed. Phenylacetic acid, 3-phenylpropionic acid, 1-naphthol, and acetophenone also showed pH-independent behavior. The buffers MES and HEPES did not affect the visible spectrum of $Ni(TF_4TMAP)Cl_4$ at pH values significantly below their pK_a's (~6.5 (MES) and 7.6 (HEPES)) but caused the porphyrin to be four coordinate in basic solution, Table 6.

---

(70) Kadish, K. M.; Maiya, B. G.; Araullo-McAdams, C. *J. Phys. Chem.* **1991**, *95*, 427.

Table 7. Effect of Substrates on the Fraction of $Ni(T(F_4TMA)P^{4+}$ Present as the Four-Coordinate Species

substrate	effect at 0.01 M	comments
terephthalate	slight interaction at pH 9	too insoluble at lower pH's
phthalate	>80% 4 coordinate at pH 4	no interaction at pH 8
phenylacetic acid	>75% 4-coordinate at pH 2	broad Soret at pH 8
phenylpropionic acid	>80% 4-coordinate at pH 2 and 8	
3-trimethylsilylpropane-1-sulfonate	50% binding at 0.001 M	
perfluorooctanesulfonate	>90% 4-coordinate at 1×10^{-5} M	precipitates at longer times
MES	70% 4-coordinate at pH 8	no interaction at pH 3
HEPES	60% 4-coordinate at pH 9	no interaction at pH 5
4-toluenesulfonate	>70% 4-coordinate	
1,3-benzenedisulfonate	>90% 4-coordinate	broad Soret; $K = (5 \pm 3) \times 10^4$ M^{-1} [a]
2,6-naphthalenedisulfonate	>90% 4-coordinate at 0.001 M	broad Soret; $K = (5 \pm 2) \times 10^4$ M^{-1} [a]
acetophenone	>80% 4-coordinate	
1-naphthol	>90% 4-coordinate at pH 3 and pH 8	
cyclohexanol		$K_1 = 50 \pm 10$;[a] probable second binding

[a] Binding constants are calculated assuming binding only to the four-coordinate form and are equal to the observed constant × 2.6.

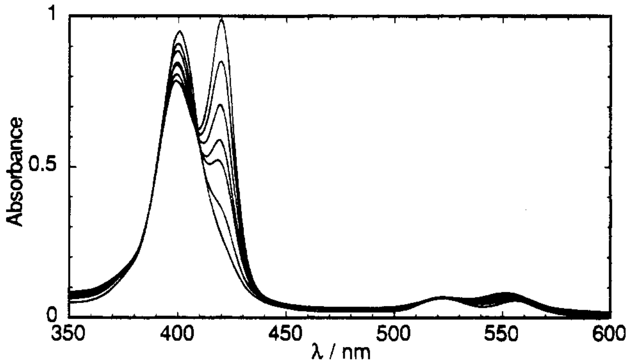

Figure 10. Titration of an aqueous solution of $NiTF_4TMAP^{4+}$ with HEPES at pH 10.01 at 25.0 °C. [HEPES] = 0.0, 0.0010, 0.0030, 0.0060, 0.010, 0.030, and 0.10 M.

A study of the displacement of coordinated water by HEPES at pH 10 showed that the absorbance change could be fit to a binding isotherm with an observed binding constant $K_{obs} = (2.0 \pm 0.3) \times 10^2$ M^{-1}, Figure 10. There was no evidence for binding of a second HEPES up to 0.1 M. The spectral changes were independent of porphyrin concentration (10^{-5}–10^{-4} M), showing that the decrease in water coordination was not due to induced porphyrin aggregation. If it is assumed that binding only occurs to the four-coordinate nickel and that at 25 °C the ratio of six- to four-coordinate nickel is 1.6:1, then the binding constant $K_1 = 2.6K_{obs} = (5.2 \pm 0.8) \times 10^2$ M^{-1}. Substrates containing two carboxylate groups showed pH-dependent perturbations of the absorption spectra of aqueous solutions of $Ni(TF_4TMAP)Cl_4$. Thus, at high pH (pH >8), terephthalic acid and potassium hydrogen phthalate did not affect the Soret region while at low pH (pH 2–5) the 420 nm band in these systems was suppressed. Ammonium perfluoro-1-octanesulfonate caused complete inhibition of aquation of the nickel even at concentrations less than 10^{-5} M. In addition, perfluoro-1-octanesulfonate (10^{-4} M) displaced 1-methylimidazole (0.1 M) from the porphyrin. However, further study of the interaction with perfluoro-1-octanesulfonate was complicated by the subsequent precipitation of the porphyrin.

Discussion

The crystal structure shows that structurally there is little difference between this water-soluble porphyrin and related organic-soluble porphyrins. This is expected, since the charged groups are at the periphery of the molecule. This is the first crystal structure of a four-coordinate water-soluble nickel porphyrin, the previous example of a water soluble nickel porphyrin being the six-coordinate $NiT(4\text{-}NMePyP)(Im)_2(ClO_4)_4$.[53] The structure of $Ni(TF_4TMAP)(CF_3SO_3)_4{\cdot}2CH_3CN{\cdot}2(CH_3)_2CO$ clearly shows that there is no tendency for the $CF_3SO_3^-$ anions in this cationic Ni^{II} porphyrin to become axial ligands in the solid state. The porphyrin is indefinitely stable in solution and in the solid state as the $CF_3SO_3^-$ or PF_6^- salts, but in the solid state the chloride salt is demethylated over a period of days.

The binding constants observed for $Ni(TF_4TMAP)^{4+}$ are significantly higher than those observed for $Ni(TF_4DMAP)$, in accord with earlier studies on substituted tetraphenylporphyrins[44,45] and 2,4-disubstituted deuteroporphyrins,[43] which showed that ligand binding to nickel porphyrins is sensitive to the electron-donating or withdrawing nature of the porphyrin substituents. $Ni(TF_4TMAP)^{4+}$ is the most electron-withdrawing nickel porphyrin for which such ligand binding has been examined, and the binding constants obtained for this porphyrin are comparable with the results obtained for reduced porphyrin macrocycles such as nickel β-oxophlorin.[71] The increase in binding can be ascribed predominantly to the increased electrophilic nature of the metal due to the strongly electron-withdrawing 2,3,5,6-tetrafluoro-*N,N,N*-trimethyanilinium substituents at the meso positions of the porphyrin ring. The phenyl rings are close to perpendicular to the porphyrin plane, so that the electronic influence of the substituents is almost completely inductive. This porphyrin probably approaches the limit of purely inductive effects on *meso*-arylporphyrins, so that further perturbations will require modification of the porphyrin ring or addition of charged groups close to the porphyrin ring. The observations made here complement the earlier conclusion that high binding affinity for axial ligands in Ni(II) macrocycles is mainly due to the ability of the macrocycle to become distorted or expand to fit different-sized metal ions.[72] Ligand affinity is controlled by the total ligand field effect of the equatorial porphyrin nitrogens, and this will be controlled by both the geometry and the basicity of these nitrogens. A significant observation in the current study is the observation of ranges of stability for five-coordinate nickel complexes, particularly for stronger field ligands such as tributylphosphine. Thus at 5 mM PBu_3 in acetonitrile, approximately 76% of the Ni^{II} porphyrin is present as $[Ni(TF_4TMAP)PBu_3]^{4+}$. Other porphyrin studies have given conflicting results as to the existence of five-coordinate nickel,[43–45] and stepwise association of axial ligands has only been reported for strong field ligands such as piperidine.[45] Statistical analysis shows that since potential ligands can approach either side of the porphyrin plane, independent binding of ligands will lead to $K_1 = 4K_2$ in eqs 1

---

(71) Connick, P. A.; Haller, K. J.; Macor, K. A. *Inorg. Chem.* **1993**, *32*, 3256.

(72) Stolzenberg, A. M.; Stershic, M. T. *J. Am. Chem. Soc.* **1988**, *110*, 6391.

and 2. The binding of 1-methylimidazole to $Ni(TF_4TMAP)^{4+}$ appears to occur approximately independently using this criterion. Weaker-field ligands have similar values for K_1 and K_2, or may even bind two ligands together (i.e. $K_2 > K_1$), while stronger field ligands have $K_1 \gg K_2$ due to their increased trans influence. It is likely that for many more electron-rich porphyrins, such as most of the organic-soluble species, the porphyrin ligand field is sufficiently strong that most axial ligands behave as the weaker ones do in this study, and form only four- and six-coordinate species.

Our results in aqueous solution show that $Ni(TF_4TMAP)^{4+}$ is monomeric in aqueous solution, and that a greater proportion of the porphyrin is six-coordinate (two axial waters) than is the case for $Ni(T4\text{-}NMePyP)^{4+}$. The behavior was monitored primarily using NMR and UV−visible spectroscopy. There have been claims that these techniques are unable to detect a monomer−dimer equilibration for $H_2(T4\text{-}NMePyP)^{4+}$, which would cast doubt on the validity of studies such as the present one. We therefore reexamined the chemistry of $H_2(T4\text{-}NMePyP)^{4+}$, both by duplicating reported UV−visible and fluorescence measurements and by testing the hypothesis of a dimerization under conditions of competing equilibria. All of our results show that the maximum value for the purported dimerization constant is 2×10^4 M^{-1}, so that under the conditions usually used in UV−visible studies (concentrations less than 10^{-4} M) $H_2(T4\text{-}NMePyP)^{4+}$ is monomeric in aqueous solution. There was no evidence for association of the nickel porphyrin in the present study except in the presence of hydrophobic organic substrates such as perfluorooctanesulfonate and tetraphenylborate, so that all the aqueous chemistry is of the monomeric species.

The interactions of organic substrates with $Ni(TF_4TMAP)^{4+}$ in aqueous solution can be followed by monitoring the decrease in the amount of six-coordinate axially-ligated porphyrin. The results obtained show that both aromatic and aliphatic substrates can interact with the porphyrin. Furthermore, the interaction is decreased by the presence of two or more negative charges even though the porphyrin is tetracationic. Thus, hydrogenphthalate inhibits the formation of the diaquo nickel porphyrin, but phthalate has little effect, and terephthalate causes very little change in the visible spectrum. We ascribe the reduction in interaction to increased hydration of the substrate, rather than to any effect on the porphyrin. The fact that 1,3-benzenedisulfonate does interact with the porphyrin suggests that here the benzene ring can partially overlap with a face of the porphyrin. The present results show that the contribution of ionic interactions is minor, in contrast to interpretations by a previous study which followed the interaction between water-soluble porphyrins and organic substrates using NMR.[30] A possible reason for the difference is that the NMR study looked at shifts in the substrates due to interaction with the porphyrin, and this could occur both for close-contacting and solvent-separated species, while our measurement only detects the close-contacting species in which water is displaced from the nickel center. The observation that aliphatic species such as HEPES, MES, perfluorooctanesulfonate, and cyclohexanol and, to a lesser extent, acetone and acetonitrile interact with this porphyrin in aqueous solution shows that interactions of porphyrins with organic species in aqueous solution should not be ascribed purely to $\pi-\pi$ interactions,[31] but rather that more general hydrophobic interactions play a significant role. This is especially true for this fluorinated porphyrin, but will be true for other water-soluble porphyrins as well. Thus, porphyrin interactions with biological macromolecules should be treated as occuring via a combination of ionic interactions, $\pi-\pi$ interactions with aromatic residues and a more general hydrophobic interaction.

Conclusion

Our studies demonstrate that $Ni(TF_4TMAP)^{4+}$ is very similar structurally to other nickel porphyrins and that the ligand binding properties in organic solvents are well-explained by extrapolation from other, less electron-withdrawing nickel porphyrins such as $Ni(TF_4DMAP)$ and substituted NiTPP's. However, when the chemistry of this porphyrin is studied in water then the hydrophobic effect of the fluorine substituents becomes important. Addition of small amounts of organic solvents or water-soluble organic molecules causes the displacement of axial water from six-coordinate nickel porphyrins to form the square-planar four-coordinate nickel species. This must occur via association of the organic substrates and the porphyrin ring. This association can be described as selective solvation for solvents such as acetone and acetonitrile and could be ascribed to $\pi-\pi$ bonding for aromatic substrates. Our study also shows that ion-pair interactions are not as important for binding *when binding is measured by examining the hydration of the central metal in a porphyrin.* In fact, increase of the charge on a substrate *decreases* the apparent binding, probably due to the increased hydration of the substrate. The fact that association is seen for substrates such as HEPES, MES, and cyclohexanol suggests that association is driven by the general hydrophobic effect. Here the term hydrophobic effect is used to refer to the preference of water molecules to bond to water rather than to non-polar solutes, which leads to association of solutes even if the direct intermolecular forces between the solutes are small.[32,33] This effect is increased in importance for this fluorinated porphyrin compared to other water-soluble porphyrins. However, models of porphyrin interactions with biological substrates should take the hydrophobic effect into account as well as any other more specific interactions.

Acknowledgment is made to the donors of the Petroleum Research Fund, administered by the American Chemical Society, for the partial support of this work. Funds for the rotating-anode diffractometer were provided in part from NSF Instrument Grant CHE-92-16167. This work was also supported by a ZRIF grant from the University of Southern California and a grant from Professor A. B. Burg. The authors thank Professor A. W. Adamson for the use of his spectrofluorimeter. T.L. acknowledges support by a grant from the Department of Education, National Needs program.

Note Added in Proof. A recent paper (Vergeldt, F. J.; Koehorst, R. B. M.; Van Hoek, A.; Schaafsma, T. J. *J. Phys. Chem.* **1995**, *99*, 4397) reports complementary experiments indicating the monomeric nature of $H_2T4\text{-}N\text{-}MePyP^{4+}$. In addition, this paper suggests a mechanism for the difference between the fluorescence spectrum of $H_2T4\text{-}N\text{-}MePyP^{4+}$ measured in water and that measured in organic solvents.

Supporting Information Available: Complete listings of bond lengths (Table S1), bond angles (Table S2), and anisotropic displacement coefficients (Table S3) (7 pages). Ordering information is given on any current masthead page.

IC9501125